

# Proc3D: Procedural 3D Generation and Parametric Editing of 3D Shapes with Large Language Models

Fadlullah Raji<sup>1</sup>, Stefano Petrangeli<sup>2</sup>, Matheus Gadelha<sup>2</sup>, Yu Shen<sup>2</sup>, Uttaran Bhattacharya<sup>2</sup>, Gang Wu<sup>2</sup>

<sup>1</sup>University of South Florida

<sup>2</sup>Adobe Research

fraji@usf.edu, {gadelha, shenyu, petrange, ubhattach, gawu}@adobe.com

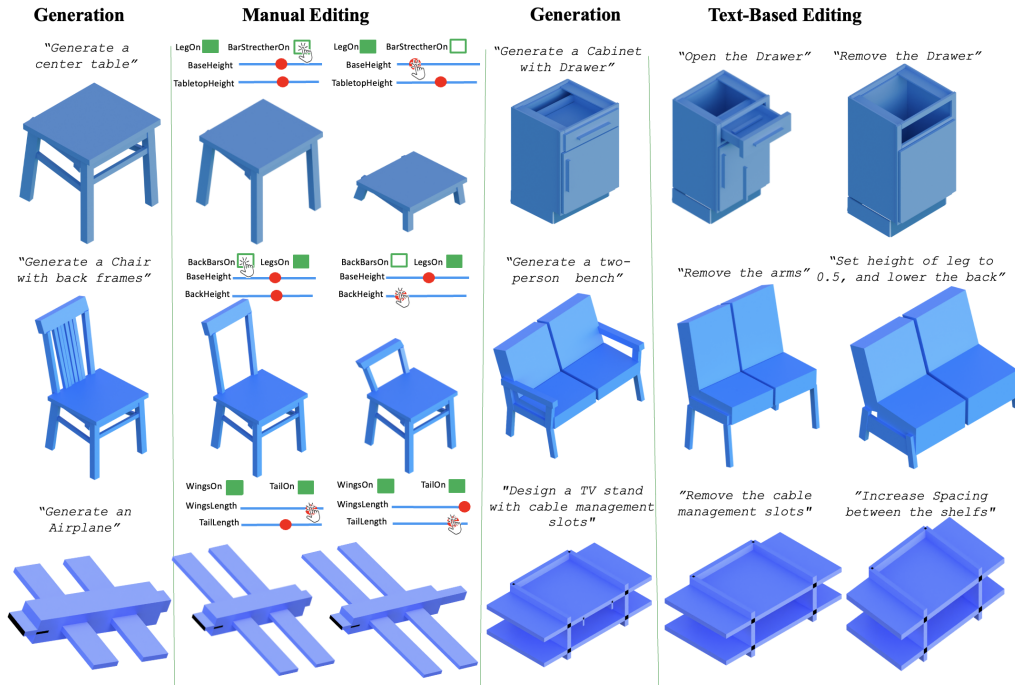


**Figure 1: Qualitative results of Proc3D.** Proc3D facilitates the generation of editable 3D models, and relative parameters from Large Language Models (LLMs) using Procedural Compact Graph (PCG) representation, which provides an efficient, compact, and editable graph-based structure for 3D models. These graphs can be directly modified in real time, using intuitive manual controls, such as sliders and checkboxes. Additionally, Proc3D enables text-based editing of the PCG with the assistance of the LLM, allowing users to make modifications through concise or detailed natural language instructions.

## Abstract

Generating 3D models has traditionally been a complex task requiring specialized expertise. While recent advances in generative AI have sought to automate this process, existing methods produce non-editable representation, such as meshes or point clouds, limiting their adaptability for iterative design. In this paper, we introduce Proc3D, a system designed to generate editable 3D models while enabling real-time modifications. At its core, Proc3D introduces procedural compact graph (PCG), a graph representation of 3D models, that encodes the algorithmic rules and structures necessary for generating the model. This representation exposes key parameters, allowing intuitive manual adjustments via sliders and checkboxes, as well as real-time, automated modifica-

tions through natural language prompts using Large Language Models (LLMs). We demonstrate Proc3D's capabilities using two generative approaches: GPT-4o with in-context learning (ICL) and a fine-tuned LLAMA-3 model. Experimental results show that Proc3D outperforms existing methods in editing efficiency, achieving more than **400x speedup** over conventional approaches that require full regeneration for each modification. Additionally, Proc3D improves ULIP scores by 28%, a metric that evaluates the alignment between generated 3D models and text prompts. By enabling text-aligned 3D model generation along with precise, real-time parametric edits, Proc3D facilitates highly accurate text-based image editing applications.

## Introduction

High-quality 3D modeling remains a labor-intensive task requiring specialized expertise. Recent text-driven generative AI can produce point clouds (Nichol et al. 2022; Hwang et al. 2023), meshes (Tsalicoglou et al. 2024; Michel et al. 2022; Siddiqui et al. 2023), implicit fields (Jun and Nichol 2023; Li et al. 2023; Cheng et al. 2023), and other representations (Poole et al. 2023; Lu et al. 2024; Lin et al. 2023; Chen et al. 2023). However, these formats are inherently static: point clouds lack explicit connectivity for targeted edits; meshes demand costly re-meshing or constraint solving for even minor changes (Fröhlauf et al. 2024; Achlioptas et al. 2023); and implicit or neural fields do not expose human-interpretable parameters, making iterative refinement and localized adjustments cumbersome. Procedural 3D modeling, where shapes are defined by parametric operations and algorithmic rules offers dynamic control and precise editability (Pearl et al. 2022; Greff et al. 2022; He et al. 2021; Deitke et al. 2022; Raistrick et al. 2023; Sun et al. 2024; Zhou et al. 2024). Yet crafting procedural programs demands deep domain knowledge, and existing AI-driven approaches focus on driving predefined procedural templates (Pearl et al. 2022; Sun et al. 2024; Zhou et al. 2024; Stekovic et al. 2024), constraining user creativity to limited parameter ranges.

In this work, we present **Proc3D**, a unified system for generating and editing procedural 3D graphs directly from text. At its core is the *Procedural Compact Graph (PCG)*, a language-native, engine-agnostic graph representation that encodes 3D objects as a compact sequence of high-level operations, exposes editable parameters on each node for true real-time, localized edits via GUI controls or natural-language follow-ups, and compiles seamlessly to multiple runtimes without API-specific dependencies. We collect a mesh-derived PCG-instruction pairs and fine-tune a LLaMA-3 model for robust PCG generation. Our evaluations show that Proc3D achieves 4–10× more compact representations than code-based DSLs (Table 1); improves ULIP alignment by 28% over text-to-3D baselines (Table 2); enables local edits 400× faster than full-regeneration methods, and maintains strong in-distribution and out-of-distribution performance with detailed ablations on LLM choices and interpreter latency.

### Our contributions are as follows:

- We develop Proc3D, a system that enables 3D generation from high-level text input and intuitive edit of 3D models through a compact graph representation.
- We introduce a compact and efficient representation of procedural 3D graphs that simplifies their inherent complexity, termed *procedural compact graph (PCG)*.
- To enable robust training and evaluation, we curate a large dataset of procedural 3D graphs along with corresponding instructions, and fine-tune a trained LLaMA-3 model for robust generation of 3D models.

## Related Work

**Text to 3D Shape Generation.** Text-to-3D generation has seen significant advancements, with various methods improving different aspects of the process. Early approaches like

CLIP-Mesh (Khalid et al. 2022) utilized CLIP (Radford et al. 2021) model for zero-shot 3D synthesis. Since then, several works have rapidly advanced the generation of 3D objects using meshes (Tsalicoglou et al. 2024; Michel et al. 2022; Siddiqui et al. 2023) and signed distance fields (SDF) (Cheng et al. 2023; Li et al. 2023). Text-guided methods have also evolved rapidly, particularly through score distillation sampling (SDS) (Poole et al. 2023; Lin et al. 2023; Chen et al. 2023; Tang et al. 2023; Wang et al. 2023), which distills pre-trained text-to-image diffusion models to improve quality and text-to-3D alignment. Despite these advancements, the representations through which these 3D models are generated, makes control and editing difficult. Proc3D introduces Procedural Compact Graph (PCG), a language-native graph of high-level operations that LLMs can generate and parse. Unlike static mesh or implicit-field methods, PCG inherently exposes node-level parameters for targeted, real-time edits without requiring full regeneration.

**Procedural 3D Modeling.** Procedural modeling has long been pivotal for generating structures like plant models (Prusinkiewicz and Lindenmayer 1996; Gasch et al. 2022) and urban environments (Parish and Müller 2001; Müller et al. 2006), often via procedural graphs which may also be used to generate natural scenes (Gasch et al. 2022; Zhang et al. 2019) and cityscapes (Lipp et al. 2011; Yang et al. 2013; Vanegas et al. 2012; Talton et al. 2011). Tools like Blender offer drag-and-drop graph construction, but extensive parameter tuning remains labor-intensive. Recent generative AI approaches help automate some aspects: ShapeAssembly (Jones et al. 2020) uses code-to-code interpolation, Geocode (Pearl et al. 2022) maps sketches or point clouds to parametric graphs, and Infinigen (Raistrick et al. 2023) generates infinite landscapes and indoor scenes (Raistrick et al. 2024). Large language models have also been used to reduce manual editing (Zhou et al. 2024; Sun et al. 2024), but procedural graph creation itself still relies heavily on manual creation, limiting their broader automation. Our work is the first to enable direct generation of procedural 3D graphs from text instructions, opening new avenues for 3D modeling.

**Large Language Models for 3D Generation.** Large language models (LLMs) encode vast knowledge into language-based representations, enabling broad applicability across tasks (Raffel et al. 2020; Bubeck et al. 2023; Chowdhery et al. 2022; OpenAI 2024; Devlin et al. 2019). Initially developed for text, LLMs now extend to mathematical reasoning (Wei et al. 2022; Imani, Du, and Shrivastava 2023), planning (Song et al. 2023; Huang et al. 2022; Zhao, Lee, and Hsu 2023), and code generation (Chen et al. 2021; Rozière et al. 2024), motivating their adaptation for 3D content creation. However, 3D generation remains fundamentally difficult due to the spatial, hierarchical, and topological complexity of geometric data. Recent works have explored mesh-based and procedural approaches, but limitations remain. Autoregressive models like MeshXL (Chen et al. 2024) and LLaMA-Mesh (Wang et al. 2024) serialize geometry as vertex-face sequences, which are difficult to edit or interpret in natural language. Procedural methods such as 3D-GPT (Sun et al. 2024) and SceneCraft (Hu et al. 2024) rely on fixed templates

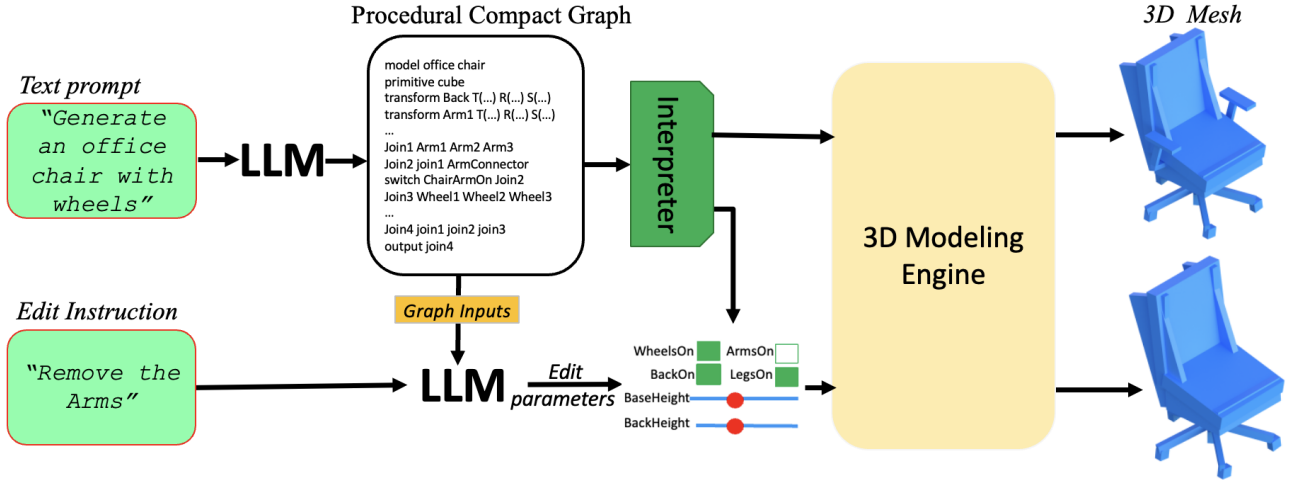


Figure 2: **3D Generation and Editing Pipeline.** Given a text prompt, a Large Language Model (LLM) constructs the Procedural Compact Graph (PCG), which is interpreted into software-specific formats suitable for 3D modeling engine such as Blender or Unity3D. Subsequent edits submitted via text prompt are integrated by the LLM to update the graph and, consequently, the 3D mesh.

or asset libraries with limited parameter control, constraining expressiveness. BlenderAlchemy (Huang, Yang, and Guibas 2024) enables vision-language editing of 3D scenes but lacks support for generative modeling from scratch. Meanwhile, L3GO (Yamada et al. 2024) and 3D-Premise (Yuan et al. 2024) generate Blender Python code via prompting, but are tightly coupled to Blender’s engine and produce verbose, brittle scripts.

To overcome these issues, we introduce a simplified procedural modeling framework that reduces task complexity for LLMs by leveraging structured, interpretable graph representations. Our system, Proc3D, enables editable, engine-agnostic 3D generation directly from natural language prompts.

## Proc3D

**System Overview.** An overview of our system is shown in Figure 2. The system facilitates both generation and intuitive editing of procedural 3D models using natural language inputs, by leveraging LLMs and a compact representation for procedural 3D graphs. At the core of the system is *Procedural Compact Graph (PCG)*, a simplified language designed to reduce the complexity of traditional procedural modeling, and making it feasible for LLMs to efficiently generate and interpret 3D models.

To generate 3D models, users provide natural language instructions, which are then translated into the corresponding procedural representation. This representation is decoded into input parameters, such as booleans to toggle parts or continuous values to adjust dimensions. A software-specific interpreter converts the graph into executable code—such as Python scripts for Blender—where the 3D model is rendered. Users can perform parametric edits using sliders or checkboxes linked to the input parameters, or automated edit via additional natural language commands (e.g., "Make the legs taller"), enabling real-time modifications.

In the following subsections, we detail our contributions:

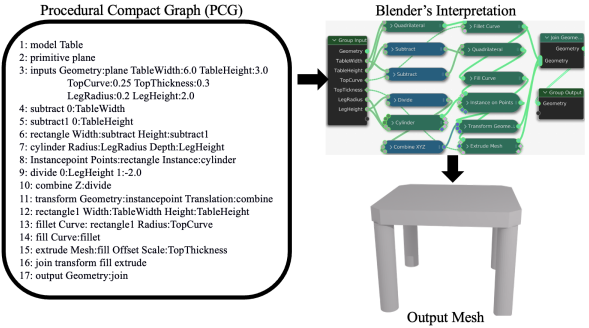


Figure 3: **An example of the procedural compact graph (PCG).** Each line is a node in the procedural 3D graph that defines the operation performed on the connected node. The graph is interpreted into blender’s geometric node where the mesh can be visualized.

the design of the *Procedural Compact Graph (PCG)*, the translation of 3D meshes into PCG for large dataset curation, and the process of generating and editing 3D models via natural language inputs.

## Procedural Compact Graph (PCG)

In traditional 3D modeling software like Blender, users create procedural 3D models by connecting geometric nodes through a drag-and-drop user interface (UI). While intuitive, these node-based graphs often become complex, especially in platform-specific code formats, creating challenges for LLMs due to context length limitations and syntax errors (Li et al. 2024). To address this, we propose the Procedural Compact Graph (PCG), a simplified representation that abstracts procedural operations into a concise format, reducing context overhead by 4-10X compared to platform-specific codes. For example, the PCG example shown in Figure 3 achieves a 5X reduction over Infinigen’s code (Raistrick et al. 2023) (see supplementary material) and over 10X compared to Blender’s

Python code for the same 3D mesh. Each PCG line represents a node or operation with defined parameters and connections, simplifying 3D model generation and interpretation by LLMs. Detailed node definitions are provided in the supplemental material. Next, we describe how to extract this representation from hierarchically segmented 3D meshes.

**Extracting PCG from 3D Meshes.** Procedural 3D graphs effectively represent parametric 3D shapes but are complex to generate, typically requiring domain experts and creating a data collection bottleneck. To address this, we repurpose hierarchically segmented 3D meshes. Our pipeline begins with a large dataset of hierarchical 3D part models (Mo et al. 2019a,b), where shapes are assemblies of parts represented as nodes. These nodes are connected by edges that signify physical attachments and hierarchical parent-child relationships, indicating how larger parts comprise smaller sub-components. Leaf nodes, or atomic parts, are represented using cuboid geometries (see Figure 4). Using the PartNet (Mo et al. 2019b) mesh dataset, we perform two key processes to extract PCG compositions, detailed below, and Pseudo-code of the extraction process in Figure 17 of the supplemental material.

**A. Recursive Combination of Parts.** To construct a procedural 3D graph from semantically segmented meshes, we recursively traverse the hierarchy from root to leaf nodes. Each node represents a terminal component (e.g., chair back, table leg) and connects to its parent via a Join Node in PCG. Multiple leaf nodes with the same semantic name, like chair legs, are merged into a single child node before attaching to the parent. The Join Node integrates these components into a cohesive model, ensuring structural integrity. Transformations applied to a parent node, such as translation or scaling, automatically propagate to child nodes, allowing consistent modifications across the entire model.

**B. Exposing Editable Properties.** At each recursive step, key properties such as rotation, scaling, and translation are exposed for precise adjustments to individual parts. Each child node includes a switch to enable or disable components, allowing seamless manipulation. For instance, toggling a chair’s armrests *on* or *off* affects all sub-components under the `armrest` label, such as padding or supports. Major structural parts, like the chair base, are adjusted as a whole rather than individually modifying legs, bar stretchers, or wheels. Changes to the base’s properties, such as height or scale, automatically propagate to related components, maintaining proportionality. This approach allows dynamic object modifications without regenerating the entire procedural graph.

**Instruction-Graph Data Collection.** Our data collection pipeline, shown in Figure 4, converts hierarchical 3D meshes from the PartNet dataset (Mo et al. 2019b) into PCG representations, resulting in 21K models across five categories: Chairs, Tables, Trash Cans, Storage Furniture, and Beds. Multi-view images of the PCG models are then rendered from front-facing cameras to capture their full geometry and structure, ensuring detailed visualization from various angles. These multi-view images are compiled into tiled images, which are analyzed by LLaVA (Liu et al. 2023) to generate detailed text descriptions, capturing attributes like shape, geometry, and spatial relationships. The captions produced by

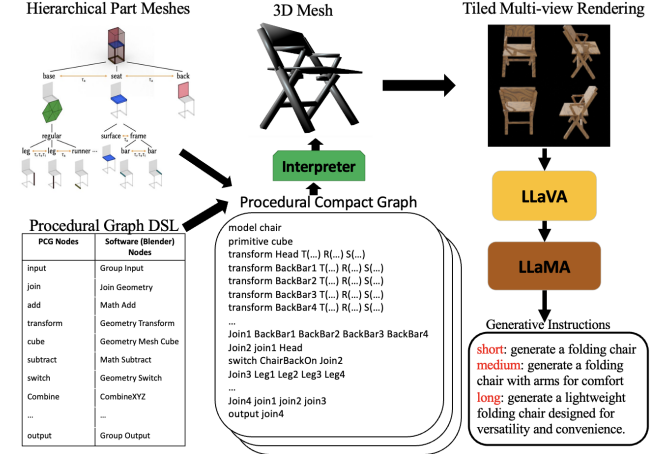


**Figure 4: Data Collection Pipeline.** Given a dataset of the hierarchical part meshes (Mo et al. 2019b,a), we extract the PCG representations, and rendered multi-view images of the 3D model. Then, using LLaVA, we collect detail caption of the rendered views, which is passed through LLaMA-3 70B for the generation of corresponding instructions.

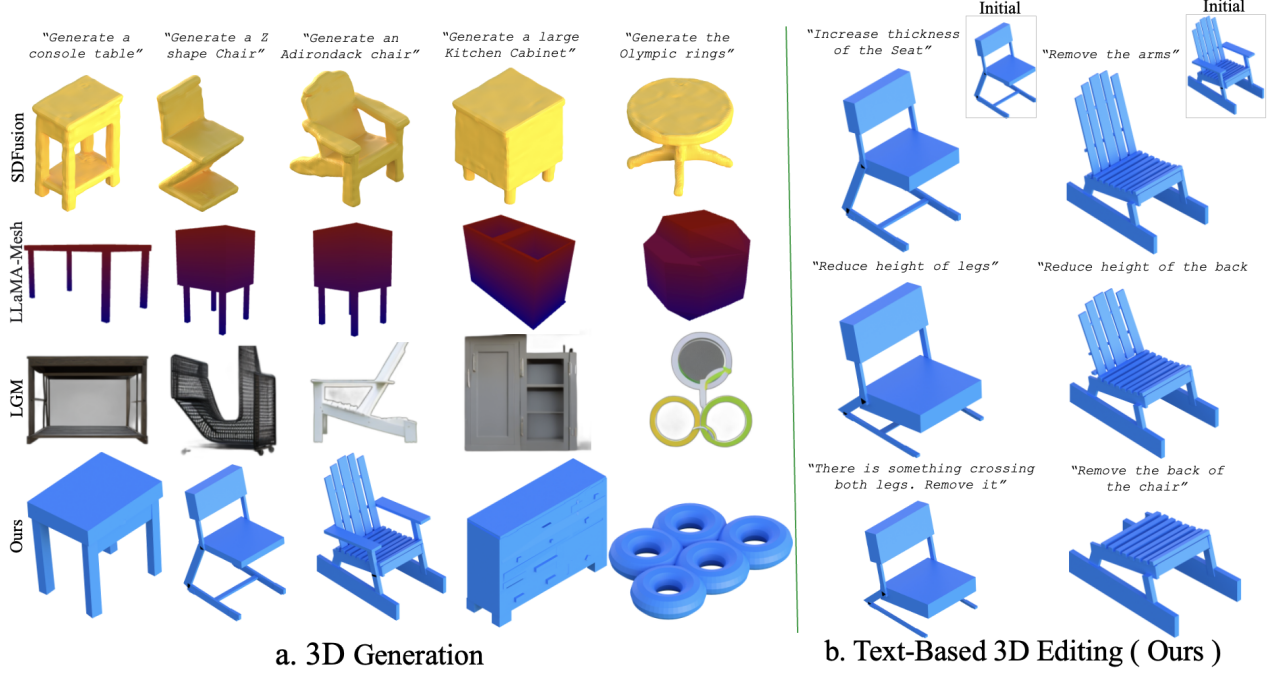
LLaVA are then processed by LLaMA-3 to generate structured generative instructions tailored to three levels of detail: *short*, providing concise summaries; *medium*, offering detailed feature descriptions; and *long*, covering comprehensive structural and contextual information. This process produces 63K instruction-graph pairs, enabling robust training and evaluation.

### 3D Generation and Parametric Edits

This subsection outlines our system’s core functionalities, leveraging LLMs for text-based generation and parametric editing of 3D objects. Users can create 3D content and interactively modify object parameters via natural language. This interaction is facilitated by PCG, which serves as an intermediary representation of the object’s geometric structure and connectivity. The graph-based approach ensures that generated objects remain parametric and adaptable throughout their lifecycle.

**3D Object Generation.** The generation process starts with a user-provided text prompt processed by the LLM. For example, a prompt like “Generate an office chair with wheels” is interpreted by the model to construct the corresponding PCG, which encodes the object’s geometric and topological properties, including part connectivity, transformations, and relationships. This PCG is then passed to an interpreter that converts it into a software-specific format compatible with modeling environments like Substance 3D, Blender, or Unity. The interpreter maps the procedural definitions to commands understood by these platforms, making the graph’s geometric instructions executable.

**Parametric Edits and Interactive Modification.** Our system supports robust parametric editing, enabling users to modify objects manually or via text-based instructions. Edits



a. 3D Generation

b. Text-Based 3D Editing ( Ours )

Figure 5: **Comparative Analysis of 3D Object Generation and Editing.** (a) 3D Generation: Comparison of different methods for generating 3D models from text prompts, including SDFusion (Cheng et al. 2023), LLaMA-Mesh (Wang et al. 2024), LGM (Tang et al. 2024), and our proposed method (Ours). Our method achieves more consistent, structured outputs across various prompts. (b) Text-Based 3D Editing: Our system introduces representation that enabled targeted edits on the generated 3D objects from text prompts. Other methods do not support editing the generated 3D models.

are applied at the PCG level, ensuring structural coherence and preserving the object’s integrity. For example, a command like “Remove the arms” prompts the LLM to update relevant PCG parameters, such as removing components or adjusting transformation parameters. The graph-based structure ensures precise and efficient modifications, as changes to one component automatically update related transformations to maintain consistent geometry. The updated PCG is then recompiled into a software-specific representation for immediate visualization, enabling real-time iterative design through successive text inputs.

## Experiment

We present experiments to evaluate the generation, and editing of procedural 3D models from our framework. For these experiments, we utilize both GPT-4o(OpenAI 2024) and the LLaMA models (8B and 70B parameters) (Dubey et al. 2024).

**Datasets.** To enable few-shot ICL, we manually annotated 1,000 examples, where humans observed rendered 3D objects and provided generative instructions (e.g., “a table with a single central leg”). For the remaining graphs in the dataset, we applied the automated method outlined in .

**Evaluation Metrics.** To evaluate the effectiveness of our proposed system, we utilize three primary metrics: *Compile Rate* to assess how often the generated 3D procedural graphs

Table 1: **Comparative Performance of LLM-Generated Representations.** PCG representation demonstrates superior abstraction with the highest compile rate and the lowest generation time, highlighting significant advancements in efficiency and capability.

Representation	Compile Rate (%)	Avg. Token Length	Gen. Time (s)
Blender Geo. Node	0	6048	62
Infinigen(Raistrick et al. 2023)	5	3403	50
Blender Code (Yuan et al. 2024)	30	2789	43
LLaMA-Mesh (Wang et al. 2024)	45	3189	25
<b>PCG (Ours)</b>	<b>89</b>	<b>702</b>	<b>9</b>

are syntactically correct and can be successfully compiled. *Similarity Measure* to quantify the geometric similarities between the generated and the closest reference 3D models in the training data. Lastly, the *ULIP* (Unified Language and Image Pre-training) (Xue et al. 2022) score assesses the perceptual loss between the input text prompt and the generated shape, thus providing insight into the alignment between the 3D shape and the input prompts.

**Baselines.** We benchmark our proposed system against several established models in both 3D and 2D image generation and editing: *SDFusion* (Cheng et al. 2023), a latent diffusion-based model for generating 3D shapes through signed distance functions; *AutoSDF*(Mittal et al. 2022), which leverages a 3D autoencoder and BERT (Devlin et al. 2019) to

Table 2: **Comparison of ULIP Scores and Inference Time Across Methods.** Our approach using finetuned LLaMA models (L-70B-F and L-8B-F) and non-finetuned GPT-4o achieves the highest ULIP score, outperforming SDFusion, AutoSDF, Shap-E, and LLaMA-Mesh.

Method	Editable	ULIP $\uparrow$	Gen. Time $\downarrow$	Edit Time $\downarrow$
SDFusion (Cheng et al. 2023)	$\times$	0.11	8s	8s
AutoSDF (Mittal et al. 2022)	$\times$	0.07	<b>4s</b>	4s
Shap-E (Jun and Nichol 2023)	$\times$	0.10	30s	30s
LLaMA-Mesh (Wang et al. 2024)	$\times$	0.08	25s	25s
<b>Ours (L-70B-F)</b>	$\checkmark$	<b>0.15</b>	47s	<b>0.01s</b>
<b>Ours (L-8B-F)</b>	$\checkmark$	0.13	10s	<b>0.01s</b>
<b>Ours (GPT-4o)</b>	$\checkmark$	0.14	9s	<b>0.01s</b>

generate signed distance fields; *shap-E*(Jun and Nichol 2023), designed for generating conditional 3D implicit functions; LLaMA-Mesh (Wang et al. 2024), enables 3D generation from LLM by tokenizing the vertices and faces of the 3D meshes; *LGM*(Tang et al. 2024) (Large Multi-View Gaussian Model), which combines a pretrained 2D diffusion model with a large Gaussian model to generate 3D Gaussian representation of the model; *Stable Diffusion*(Rombach et al. 2022), a leading image generation model, used as a baseline for evaluating image synthesis from text input; *TurboEdit*(Deutch et al. 2024), a diffusion-based model that edits 2D based on text prompts, serving as a reference for comparing the 2D editing capabilities of our system against conventional 2D approaches; and *InstructPix2Pix*(Brooks, Holynski, and Efros 2023), a text-driven 2D image editing model with stable diffusion backbone.

## Experimental Details

Proc3D enables any LLM to generate 3D objects using our novel PCG representation. To test its flexibility, we evaluate four models: GPT-4o and LLaMA 3-70B using in-context learning (ICL), and fine-tuned variants of LLaMA 3 with 8B and 70B parameters. For ICL, 20 examples were retrieved via BM25 ranking (Amati 2009) from the instruction-graph examples, and were passed into the model, together with instruction prompts. For a robust evaluation, we used QLORA to fine-tune LLaMA-3 8B and LLaMA-3 70B for 5 epochs using our curated instruction-graph dataset, with a 90%/10% split for training and validation.

To comprehensively assess performance, we sampled 100 in-distribution (IID) and 100 out-of-distribution (OOD) unique prompts from GPT-4o, covering object categories both seen and unseen during training. These prompts were used consistently across all quantitative evaluations. This approach allowed us to fairly compare the models’ performance and evaluate their ability to generalize to new prompts.

## Quantitative Results

**3D Representation.** The PCG representation is developed to address the inefficiencies of previous LLM-compatible representation such as the blender’s geometric nodes, Infinigen (Raistrick et al. 2023) abstraction, and the python code in Blender(gd3kr and Phillips 2023; Hu et al. 2024; Yamada

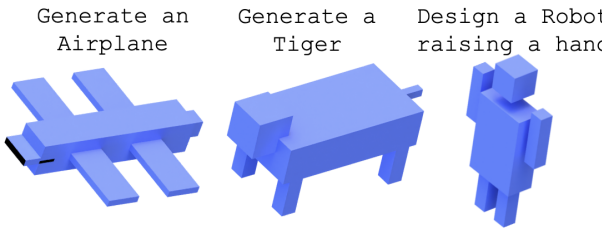


Figure 6: **Generation out of training classes.** With training data limited to chairs, tables, beds, and storage, Proc3D can generate complex 3D categories that are not in the training examples.

et al. 2024). In Table 1, we compare generation of these representations with 100 example prompts using GPT-4o with 128K context length. Results show that, by optimizing the representation of the 3D model, compile rates significantly increases, enhancing the effectiveness and efficiency of procedural generation. This advancement not only ensures more reliable outputs but also supports the use of a higher number of ICL examples for non-finetuned LLMs. We also compare these representations using more recent reasoning-oriented LLM, as shown in Table 4 of the supplementary material, to highlight their impact on compilation performance and generalization.

**3D Generation.** We present a quantitative comparison of Proc3D with the baselines in Table 2. Proc3D achieves the highest ULIP score, demonstrating superior alignment between text prompts and the generated 3D models compared to baseline methods. This result suggests that Proc3D excels at interpreting and translating text descriptions into accurate 3D representations, capturing detailed geometry and structural details with higher precision than the baselines. Notably, Proc3D with GPT-4o achieves generation times similar to those of the highest-quality previous work (Cheng et al. 2023) while enabling real-time editing of the 3D model, which is 400x more efficient than the baselines which require regenerating the 3D model and optimizing input prompts to produce the desired 3D output.

**Ablation Studies.** In Table 3, we compare LLMs for 3D model generation using Compile Rate and Similarity Measure across both few-shot ICL and fine-tuned settings. Fine-tuned models achieve higher Compile Rates, reflecting better syntactic understanding of PCG, but tend to overfit, leading to lower Similarity on out-of-training categories. Despite this, their higher ULIP scores indicate more semantically accurate outputs. For instance, LLaMA-8B underperforms GPT-4o in ULIP, highlighting the impact of overfitting on generalization. Further ablation to assess the effect of ICL example count on PCG quality is shown in the supplementary material.

**3D Editing.** Quantitative comparisons of 3D editing methods are challenging due to the lack of publicly available benchmarks and accessible implementations of alternative methods. For example, we could not access the code for methods like ParSEL (Ganeshan et al. 2024), which reportedly

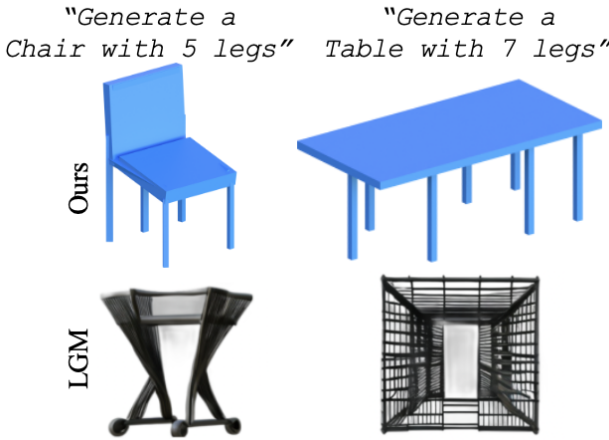


Figure 7: **Unconventional Object Generation.** Proc3D can follow the text prompt to generate unconventional objects better than LGM(Tang et al. 2024)

take 30 to 500 seconds per mesh edit. In contrast, as shown in Table 2, and in the Figure 11 Proc3D achieves edits in under 10 milliseconds, significantly outperforming these methods (**over 400x speedup**). This performance enables real-time 3D object modifications, making Proc3D a highly practical tool for dynamic 3D editing workflows.

## Qualitative Results

**3D Generation.** We present qualitative results of 3D generation in Figure 1, which demonstrate Proc3D’s ability to generate 3D models from text inputs. Figure 5 further shows the flexibility of Proc3D in generating a wide varieties of 3D shapes, from everyday objects like chairs and tables to abstract forms like the Olympic rings. Compared to baseline models, Proc3D exhibits a clear advantage in maintaining geometric consistency and capturing precise details.

We also show out-of-distribution generation examples in Figure 6. Due to the nature of our training dataset, which consists solely of cube primitives, the generated objects, in-

Table 3: **Evaluation of few-shot and fine-tuned models on both in-training (In-tr.) and out-of-training (Out-tr.) data categories.** Fine-tuned models achieve higher compile rates, but tend to lack the generalization capabilities of non-fine-tuned models. However, they consistently follow the text prompts and generate higher quality models, resulting in higher ULIP scores compared to few-shot models.

Model	Compile Rate↑		Similarity Measure↑		ULIP↑	
	In-tr.	Out-tr.	In-tr.	Out-tr.	In-tr.	Out-tr.
<b>Few-Shot ICL</b>						
GPT4o	0.89	0.86	<b>0.58</b>	0.97	0.14	0.10
llama3-70B	0.75	0.68	0.56	0.86	0.13	0.07
o3	<b>0.94</b>	<b>0.92</b>	0.62	<b>0.98</b>	<b>0.15</b>	<b>0.13</b>
DeepSeek-V3	0.92	0.91	<b>0.64</b>	<b>0.98</b>	0.14	0.11
<b>Finetuned</b>						
llama3-8B	<b>0.98</b>	<b>0.97</b>	0.46	0.49	0.13	0.06
llama3-70B	<b>0.98</b>	0.96	0.50	0.58	<b>0.15</b>	0.08

cluding more complex ones like Tigers or Airplanes, are still composed of cube-based structures. In particular, generating such out-of-distribution objects is not directly possible with traditional code-representation methods (Yuan et al. 2024; Yamada et al. 2024) or vertices-faces generation from LLM (Wang et al. 2024) without our simplified PCG language, which enables LLM to effectively reason about these models. To further illustrate the advantages of our approach, we show the generation of unconventional objects in Figure 7 and compare them against state-of-the-art diffusion and Gaussian representations (Tang et al. 2024). Our method consistently outperforms these baselines, demonstrating superior capability in generating even abstract shapes by following the user’s prompts.

**3D Editing.** We present edit results of our system in Figure 1, and several examples in the appendix, where Proc3D edits the generated 3D models either manually with sliders or checkboxes, or with natural language prompts. The right side of each example focuses on editing capabilities, allowing users to make precise modifications, such as removing components or adjusting dimensions, while preserving the structural integrity of the models. Compared to the other baselines in Figure 5, which use representations that are static and not inherently editable, Proc3D allows direct editing of the generated 3D models. This ability to modify the generated shapes directly, as shown in the figure, provides users with greater flexibility and control over the design process.

Editing 3D models can also significantly benefit 2D image generation and editing, as projections of 3D models can guide the image generation process (Zhang, Rao, and Agrawala 2023). Proc3D offers fine-grained 3D model editing capabilities, leveraging enhanced 3D controllability to generate more closely aligned with user requests or views. We compare our method with traditional image generation and editing methods in Figure 8, showing that our system produces that better meet users’ specifications.

## Conclusion and Discussion

In this work, we introduced Proc3D, a framework that empowers LLMs to generate and edit 3D objects through our novel Procedural Compact Graph (PCG) representation. PCG provides an efficient representation of 3D models, reducing complexity by over 4-10 times compared to traditional methods. Qualitative and Quantitative results shows that Proc3D outperforms state-of-the-art models, such as the Large Multi-view Gaussian Model (LGM) (Tang et al. 2024), in accurately following text instructions for unconventional objects (Figure 7) and atypical designs, such as the Olympic rings (Figure 5). This demonstrates Proc3D’s superior ability to interpret and respond to diverse text prompts. Additionally, our method achieves the highest ULIP scores, indicating strong alignment between input prompts and generated 3D models, surpassing baselines like SDFusion, AutoSDF, LLaMA-Mesh and shap-E.

**Limitation and Future Direction.** Proc3D demonstrates strong capabilities in both the generation and editing of 3D models and scenes using a procedural graph representation.



**Figure 8: Comparison of Image Generation and Editing Capabilities.** The top two rows is our system, Proc3D, which generates 3D meshes and corresponding 2D from text prompts, followed by interactive editing capabilities on the generated 3D, and consequently the 2D image. The bottom rows compare various baseline methods: Stable Diffusion (Rombach et al. 2022) for image generation, TurboEdit(Deutch et al. 2024) and Instruct-pix2pix(Brooks, Holynski, and Efros 2023) for image editing.

The model generalizes well to unseen structures and shapes, including non-trivial forms such as the Olympic rings composed of toroidal elements (Figure 6). This suggests that the learned representation is not tightly coupled to specific geometric templates. However, the diversity of current training data remains limited, as existing datasets predominantly feature low-complexity primitives. In the future, we aim to further enrich the diversity and complexity of procedural training data to support broader generalization across categories, primitives, and scene compositions.

## References

Achlioptas, P.; Huang, I.; Sung, M.; Tulyakov, S.; and Guibas, L. 2023. ShapeTalk: A Language Dataset and Framework for 3D Shape Edits and Deformations. In *CVPR*.

Amati, G. 2009. BM25. In Liu, L.; and Özsü, M. T., eds., *Encyclopedia of Database Systems*, 257–260. Boston, MA: Springer. ISBN 978-0-387-35544-3.

Brooks, T.; Holynski, A.; and Efros, A. A. 2023. Instruct-Pix2Pix: Learning to Follow Image Editing Instructions. In *CVPR*.

Bubeck, S.; Chandrasekaran, V.; Eldan, R.; Gehrke, J.; Horvitz, E.; Kamar, E.; Lee, P.; Lee, Y. T.; Li, Y.; Lundberg, S.; Nori, H.; Palangi, H.; Ribeiro, M. T.; and Zhang, Y. 2023. Sparks of Artificial General Intelligence: Early Experiments with GPT-4. *arXiv preprint arXiv:2303.12712*.

Chen, M.; Tworek, J.; Jun, H.; Yuan, Q.; de Oliveira Pinto, H. P.; Kaplan, J.; Edwards, H.; Burda, Y.; Joseph, N.; Brockman, G.; Ray, A.; Puri, R.; Krueger, G.; Petrov, M.; Khlaaf, H.; Sastry, G.; Mishkin, P.; Chan, B.; Gray, S.; Ryder, N.; Pavlov, M.; Power, A.; Kaiser, L.; Bavarian, M.; Winter, C.; Tillet, P.; Such, F. P.; Cummings, D.; Plappert, M.; Chantzis, F.; Barnes, E.; Herbert-Voss, A.; Guss, W. H.; Nichol, A.; Paino, A.; Tezak, N.; Tang, J.; Babuschkin, I.; Balaji, S.; Jain, S.; Saunders, W.; Hesse, C.; Carr, A. N.; Leike, J.; Achiam, J.; Misra, V.; Morikawa, E.; Radford, A.; Knight, M.; Brundage, M.; Murati, M.; Mayer, K.; Welinder, P.; McGrew, B.; Amodei, D.; McCandlish, S.; Sutskever, I.; and Zaremba, W. 2021. Evaluating Large Language Models Trained on Code. In *arXiv*.

Chen, R.; Chen, Y.; Jiao, N.; and Jia, K. 2023. Fantasia3D: Disentangling Geometry and Appearance for High-quality Text-to-3D Content Creation. In *ICCV*, 22246–22256.

Chen, S.; Chen, X.; Pang, A.; Zeng, X.; Cheng, W.; Fu, Y.; Yin, F.; Wang, Y.; Wang, Z.; Zhang, C.; Yu, J.; Yu, G.; Fu, B.; and Chen, T. 2024. MeshXL: Neural Coordinate Field for Generative 3D Foundation Models. In *arXiv*.

Cheng, Y.-C.; Lee, H.-Y.; Tuyakov, S.; Schwing, A.; and Gui, L. 2023. SDFusion: Multimodal 3D Shape Completion, Reconstruction, and Generation. In *CVPR*.

Chowdhery, A.; Narang, S.; Devlin, J.; Bosma, M.; Mishra, G.; Roberts, A.; Barham, P.; Chung, H. W.; Sutton, C.; Gehrmann, S.; Schuh, P.; Shi, K.; Tsvyashchenko, S.; Maynez, J.; Rao, A.; Barnes, P.; Tay, Y.; Shazeer, N.; Prabhakaran, V.; Reif, E.; Du, N.; Hutchinson, B.; Pope, R.; Bradbury, J.; Austin, J.; Isard, M.; Gur-Ari, G.; Yin, P.; Duke, T.; Levskaya, A.; Ghemawat, S.; Dev, S.; Michalewski, H.; Garcia, X.; Misra, V.; Robinson, K.; Fedus, L.; Zhou, D.; Ippolito, D.; Luan, D.; Lim, H.; Zoph, B.; Spiridonov, A.; Sepassi, R.; Dohan, D.; Agrawal, S.; Omernick, M.; Dai, A. M.; Pillai, T. S.; Pellat, M.; Lewkowycz, A.; Moreira, E.; Child, R.; Polozov, O.; Lee, K.; Zhou, Z.; Wang, X.; Saeta, B.; Diaz, M.; Firat, O.; Catasta, M.; Wei, J.; Meier-Hellstern, K.; Eck, D.; Dean, J.; Petrov, S.; and Fiedel, N. 2022. PaLM: Scaling Language Modeling with Pathways. *arXiv preprint arXiv:2204.02311*.

Deitke, M.; VanderBilt, E.; Herrasti, A.; Weihs, L.; Salvador, J.; Ehsani, K.; Han, W.; Kolve, E.; Farhadi, A.; Kembhavi, A.; and Mottaghi, R. 2022. ProcTHOR: Large-Scale Embodied AI Using Procedural Generation. In *Adv. Neural Inform. Process. Syst.* Outstanding Paper Award.

Deutch, G.; Gal, R.; Garibi, D.; Patashnik, O.; and Cohen-Or, D. 2024. TurboEdit: Text-Based Image Editing Using Few-Step Diffusion Models. In *SIGGRAPH ASIA*.

Devlin, J.; Chang, M.-W.; Lee, K.; and Toutanova, K. 2019. BERT: Pre-training of Deep Bidirectional Transformers for Language Understanding. In *North American Chapter of the Association for Computational Linguistics*.

Dubey, A.; Jauhri, A.; Pandey, A.; Kadian, A.; Al-Dahle, A.; Letman, A.; Mathur, A.; Schelten, A.; Yang, A.; Fan, A.; and Others. 2024. The Llama 3 Herd of Models. In *arXiv*.

Fröhlauf, M.; Riemenschneider, H.; Gross, M.; and Schroers, C. 2024. QUADify: Extracting Meshes with Pixel-level Details and Materials from Images. In *CVPR*, 4661–4670.

Ganeshan, A.; Huang, R. Y.; Xu, X.; Jones, R. K.; and Ritchie, D. 2024. ParSEL: Parameterized Shape Editing with Language. In *arXiv*.

Gasch, C.; Sotoca, J. M.; Chover, M.; et al. 2022. Procedural modeling of plant ecosystems maximizing vegetation cover. *Multimedia Tools and Applications*, 81: 16195–16217.

gd3kr; and Phillips, F. 2023. BlenderGPT: Control Blender with Natural Language Commands Using GPT-4. <https://github.com/gd3kr/BlenderGPT>. Accessed: 2024-11-10.

Greff, K.; Belletti, F.; Beyer, L.; Doersch, C.; Du, Y.; Duckworth, D.; Fleet, D. J.; Gnanapragasam, D.; Golemo, F.; Herrmann, C.; Kipf, T.; Kundu, A.; Lagun, D.; Laradji, I.; Liu, H.-T. D.; Meyer, H.; Miao, Y.; Nowrouzezahrai, D.; Oztireli, C.; Pot, E.; Radwan, N.; Rebain, D.; Sabour, S.; Sajjadi, M. S. M.; Sela, M.; Sitzmann, V.; Stone, A.; Sun, D.; Vora, S.; Wang, Z.; Wu, T.; Yi, K. M.; Zhong, F.; and Tagliasacchi, A. 2022. Kubric: a scalable dataset generator.

He, J.; Zhou, E.; Sun, L.; Lei, F.; Liu, C.; and Sun, W. 2021. Semi-synthesis: A fast way to produce effective datasets for stereo matching. In *CVPR*, 2884–2893.

Hu, Z.; Iscen, A.; Jain, A.; Kipf, T.; Yue, Y.; Ross, D. A.; Schmid, C.; and Fathi, A. 2024. SceneCraft: An LLM Agent for Synthesizing 3D Scene as Blender Code. In *arXiv*.

Huang, I.; Yang, G.; and Guibas, L. 2024. BlenderAlchemy: Editing 3D Graphics with Vision-Language Models. In *ECCV*.

Huang, W.; Abbeel, P.; Pathak, D.; and Mordatch, I. 2022. Language Models as Zero-Shot Planners: Extracting Actionable Knowledge for Embodied Agents. In *ICML*.

Hwang, I.; Kim, H.; Lim, D.; Park, I.; and Kim, Y. M. 2023. Text2PointCloud: Text-Driven Styling for Sparse Point-Cloud. In Babaei, V.; and Skouras, M., eds., *Eurographics 2023 - Short Papers*. The Eurographics Association. ISBN 978-3-03868-209-7.

Imani, S.; Du, L.; and Shrivastava, H. 2023. MathPrompter: Mathematical Reasoning using Large Language Models. In *arXiv*.

Jones, R. K.; Barton, T.; Xu, X.; Wang, K.; Jiang, E.; Guerrero, P.; Mitra, N.; and Ritchie, D. 2020. ShapeAssembly: Learning to Generate Programs for 3D Shape Structure Synthesis. *ACM Transactions on Graphics (TOG), Siggraph Asia 2020*, 39(6): Article 234.

Jun, H.; and Nichol, A. 2023. Shap-E: Generating Conditional 3D Implicit Functions. In *arXiv*.

Khalid, N. M.; Xie, T.; Belilovsky, E.; and Tiberiu, P. 2022. CLIP-Mesh: Generating textured meshes from text using pretrained image-text models. *SIGGRAPH Asia 2022 Conference Papers*.

Li, M.; Duan, Y.; Zhou, J.; and Lu, J. 2023. Diffusion-SDF: Text-to-Shape via Voxelized Diffusion. In *CVPR*.

Li, T.; Zhang, G.; Do, Q. D.; Yue, X.; and Chen, W. 2024. Long-context LLMs Struggle with Long In-context Learning. In *arXiv*.

Lin, C.-H.; Gao, J.; Tang, L.; Takikawa, T.; Zeng, X.; Huang, X.; Kreis, K.; Fidler, S.; Liu, M.-Y.; and Lin, T.-Y. 2023. Magic3D: High-Resolution Text-to-3D Content Creation. In *CVPR*.

Lipp, M.; Scherzer, D.; Wonka, P.; and Wimmer, M. 2011. Interactive modeling of city layouts using layers of procedural content. In *Computer Graphics Forum*, volume 30, 345–354. Wiley Online Library.

Liu, H.; Li, C.; Wu, Q.; and Lee, Y. J. 2023. Visual Instruction Tuning. In *NeurIPS*.

Lu, Y.; Zhang, J.; Li, S.; Fang, T.; McKinnon, D.; Tsin, Y.; Quan, L.; Cao, X.; and Yao, Y. 2024. Direct2.5: Diverse Text-to-3D Generation via Multi-view 2.5D Diffusion. *CVPR*.

Michel, O.; Bar-On, R.; Liu, R.; Benaim, S.; and Hanocka, R. 2022. Text2Mesh: Text-Driven Neural Stylization for Meshes. In *CVPR*, 13492–13502.

Mittal, P.; Cheng, Y.-C.; Singh, M.; and Tulsiani, S. 2022. AutoSDF: Shape Priors for 3D Completion, Reconstruction and Generation. In *CVPR*.

Mo, K.; Guerrero, P.; Yi, L.; Su, H.; Wonka, P.; Mitra, N.; and Guibas, L. 2019a. StructureNet: Hierarchical Graph Networks for 3D Shape Generation. *ACM Transactions on Graphics (TOG), Siggraph Asia 2019*, 38(6): Article 242.

Mo, K.; Zhu, S.; Chang, A. X.; Yi, L.; Tripathi, S.; Guibas, L. J.; and Su, H. 2019b. PartNet: A Large-Scale Benchmark for Fine-Grained and Hierarchical Part-Level 3D Object Understanding. In *CVPR*.

Müller, P.; Wonka, P.; Haegler, S.; Ulmer, A.; and Gool, L. V. 2006. Procedural Modeling of Buildings. *ACM Transactions on Graphics (TOG)*, 25(3): 614–623. Proceedings of SIGGRAPH 2006.

Nichol, A.; Jun, H.; Dhariwal, P.; Mishkin, P.; and Chen, M. 2022. Point-E: A System for Generating 3D Point Clouds from Complex Prompts. In *arXiv*.

OpenAI. 2024. GPT-4 Technical Report. In *arXiv*.

Parish, Y. I. H.; and Müller, P. 2001. Procedural Modeling of Cities. In *Conference on Computer Graphics and Interactive Techniques*, 301–308.

Pearl, O.; Lang, I.; Hu, Y.; Yeh, R. A.; and Hanocka, R. 2022. GeoCode: Interpretable Shape Programs. In *arXiv*.

Poole, B.; Jain, A.; Barron, J. T.; and Mildenhall, B. 2023. DreamFusion: Text-to-3D using 2D Diffusion. In *ICLR*.

Prusinkiewicz, P.; and Lindenmayer, A. 1996. *The Algorithmic Beauty of Plants*. Berlin, Heidelberg: Springer-Verlag.

Radford, A.; Kim, J. W.; Hallacy, C.; Ramesh, A.; Goh, G.; Agarwal, S.; Sastry, G.; Askell, A.; Mishkin, P.; Clark, J.; Krueger, G.; and Sutskever, I. 2021. Learning Transferable Visual Models From Natural Language Supervision. In *arXiv*.

Raffel, C.; Shazeer, N.; Roberts, A.; Lee, K.; Narang, S.; Matena, M.; Zhou, Y.; Li, W.; and Liu, P. J. 2020. Exploring the Limits of Transfer Learning with a Unified Text-to-Text Transformer. *Journal of Machine Learning Research*, 21(140): 1–67.

Raistrick, A.; Lipson, L.; Ma, Z.; Mei, L.; Wang, M.; Zuo, Y.; Kayan, K.; Wen, H.; Han, B.; Wang, Y.; Newell, A.; Law, H.; Goyal, A.; Yang, K.; and Deng, J. 2023. Infinite Photorealistic Worlds Using Procedural Generation. In *CVPR*.

Raistrick, A.; Mei, L.; Kayan, K.; Yan, D.; Zuo, Y.; Han, B.; Wen, H.; Parakh, M.; Alexandropoulos, S.; Lipson, L.; Ma, Z.; and Deng, J. 2024. Infinigen Indoors: Photorealistic Indoor Scenes using Procedural Generation. In *Proceedings of the IEEE/CVF Conference on Computer Vision and Pattern Recognition (CVPR)*, 21783–21794.

Rombach, R.; Blattmann, A.; Lorenz, D.; Esser, P.; and Ommer, B. 2022. High-Resolution Image Synthesis with Latent Diffusion Models. In *CVPR*.

Rozière, B.; Gehring, J.; Gloclekle, F.; Sootla, S.; Gat, I.; Tan, X. E.; Adi, Y.; Liu, J.; Sauvestre, R.; Remez, T.; Rapin, J.; Kozhevnikov, A.; Evtimov, I.; Bitton, J.; Bhatt, M.; Ferrer, C. C.; Grattafiori, A.; Xiong, W.; Défossez, A.; Copet, J.; Azhar, F.; Touvron, H.; Martin, L.; Usunier, N.; Scialom, T.; and Synnaeve, G. 2024. Code Llama: Open Foundation Models for Code. In *arXiv*.

Siddiqui, Y.; Alliegro, A.; Artemov, A.; Tommasi, T.; Sirigatti, D.; Rosov, V.; Dai, A.; and Nießner, M. 2023. MeshGPT: Generating Triangle Meshes with Decoder-Only Transformers. In *CVPR*.

Song, C. H.; Wu, J.; Washington, C.; Sadler, B. M.; Chao, W.-L.; and Su, Y. 2023. LLM-Planner: Few-Shot Grounded Planning for Embodied Agents with Large Language Models. In *ICCV*.

Stekovic, S.; Ainetter, S.; D'Urso, M.; Fraundorfer, F.; and Lepetit, V. 2024. PyTorchGeoNodes: Enabling Differentiable Shape Programs for 3D Shape Reconstruction. *arxiv*.

Sun, C.; Han, J.; Deng, W.; Wang, X.; Qin, Z.; and Gould, S. 2024. 3D-GPT: Procedural 3D Modeling with Large Language Models. In *arXiv*.

Talton, J. O.; Lou, Y.; Lesser, S.; Duke, J.; Mech, R.; and Koltun, V. 2011. Metropolis procedural modeling. *ACM Transactions on Graphics*, 30(2): 11:1–11:14.

Tang, J.; Chen, Z.; Chen, X.; Wang, T.; Zeng, G.; and Liu, Z. 2024. LGM: Large Multi-View Gaussian Model for High-Resolution 3D Content Creation. In *ECCV*.

Tang, J.; Ren, J.; Zhou, H.; Liu, Z.; and Zeng, G. 2023. DreamGaussian: Generative Gaussian Splatting for Efficient 3D Content Creation. In *ICLR*.

Tsalicoglou, C.; Manhardt, F.; Tonioni, A.; Niemeyer, M.; and Tombari, F. 2024. TextMesh: Generation of Realistic 3D Meshes From Text Prompts. In *2024 International Conference on 3D Vision (3DV)*, 1554–1563. Los Alamitos, CA, USA: IEEE Computer Society.

Vanegas, C.; Kelly, T.; Weber, B.; Halatsch, J.; Aliaga, D.; and Müller, P. 2012. Procedural generation of parcels in urban modeling. *Computer Graphics Forum*, 31: 681–690.

Wang, Z.; Lorraine, J.; Wang, Y.; Su, H.; Zhu, J.; Fidler, S.; and Zeng, X. 2024. LLaMA-Mesh: Unifying 3D Mesh Generation with Language Models. In *arXiv preprint arXiv:2411.09595*.

Wang, Z.; Lu, C.; Wang, Y.; Bao, F.; Li, C.; Su, H.; and Zhu, J. 2023. ProlificDreamer: High-Fidelity and Diverse Text-to-3D Generation with Variational Score Distillation. In *Adv. Neural Inform. Process. Syst.*

Wei, J.; Wang, X.; Schuurmans, D.; Bosma, M.; Ichter, B.; Xia, F.; Chi, E.; Le, Q.; and Zhou, D. 2022. Chain-of-Thought Prompting Elicits Reasoning in Large Language Models. In *Advances in Neural Information Processing Systems*, volume 35, 24824–24837.

Xue, L.; Gao, M.; Xing, C.; Martín-Martín, R.; Wu, J.; Xiong, C.; Xu, R.; Niebles, J. C.; and Savarese, S. 2022. ULP: Learning Unified Representation of Language, Image, and Point Cloud for 3D Understanding. In *CVPR*.

Yamada, Y.; Chandu, K.; Lin, B. Y.; Hessel, J.; Yildirim, I.; and Choi, Y. 2024. L3GO: Language Agents with Chain-of-3D-Thoughts for Generating Unconventional Objects. In *ICLR*.

Yang, Y. L.; Wang, J.; Vouga, E.; and Wonka, P. 2013. Urban pattern: Layout design by hierarchical domain splitting. *ACM Transactions on Graphics (Proceedings of SIGGRAPH Asia 2013)*, 32.

Yuan, Z.; Lan, H.; Zou, Q.; and Zhao, J. 2024. 3D-PreMise: Can Large Language Models Generate 3D Shapes with Sharp Features and Parametric Control? In *arXiv*.

Zhang, J.; Wang, C. B.; Qin, H.; Chen, Y.; and Gao, Y. 2019. Procedural modeling of rivers from single image toward natural scene production. *The Visual Computer*, 35.

Zhang, L.; Rao, A.; and Agrawala, M. 2023. Adding Conditional Control to Text-to-Image Diffusion Models. In *ICCV*.

Zhao, Z.; Lee, W. S.; and Hsu, D. 2023. Large Language Models as Commonsense Knowledge for Large-Scale Task Planning. In *NeurIPS*.

Zhou, M.; Wang, Y.; Hou, J.; Luo, C.; Zhang, Z.; and Peng, J. 2024. SceneX: Procedural Controllable Large-scale Scene Generation via Large-language Models. In *arXiv*.

## Procedural Compact Graph (PCG)

In section 3 of the main paper, we presented, and show a full example of the PCG (see Figure 3), a representation that abstracts the complexity of software-specific representations of procedural 3D modeling. We now show the corresponding Python code using Infinigen (Raistrick et al. 2023) transpiler in Figure 18. The Blender’s native code is too long to show here. As shown, the Infinigen abstraction of the native blender’s code is significantly longer in token size compared to the concise format of PCG, highlighting the efficiency and simplicity that PCG offers. By reducing code length and complexity, PCG not only makes the modeling process more manageable but also enhances the capability of Large Language Models (LLMs) to generate and interpret 3D models effectively.

**PCG Example.** The PCG in Figure 3 of the main paper which can be interpreted and rendered by Proc3D, defines the creation of a table model. The graph begins by specifying input parameters such as *table\_width*, *table\_length*, *leg\_height*, and *leg\_radius*. It then defines the legs using *cylinder* nodes, positioned at the four corners using a *rectangle* node and a *point instance* node, with a *transform* node adjusting their placement. The tabletop is created using a *rectangle* node, beveled with a *fillet* node, smoothed using a *fill* node, and given thickness via an *extrude* node. Finally, the legs and tabletop are combined using a *join* node to output the completed model.

**Extracting the PCG from 3D Meshes** Extraction of PCG from 3D meshes involves identifying and encoding the transformations, geometric properties, and spatial relationships inherent to the model. This process requires careful analysis of each mesh element to abstract its procedural structure, allowing the PCG to represent the model in a simplified yet comprehensive format. The transformation is highlighted below:

**Transformation.** Given a 3D mesh  $\mathcal{M}$  of a leaf node in the hierarchical mesh dataset (Mo et al. 2019b) represented by vertices  $\mathbf{V} = \{\mathbf{v}_1, \mathbf{v}_2, \dots, \mathbf{v}_N\}$ , we extract the translation, rotation, and scaling transformations.

**Translation.** The translation vector  $\mathbf{T}$  is computed as the centroid of the mesh:

$$\mathbf{T} = \frac{1}{N} \sum_{i=1}^N \mathbf{v}_i$$

**Rotation.** The rotation is extracted by computing the principal axes through PCA. First, we compute the covariance matrix:

$$C = \frac{1}{N} \sum_{i=1}^N \mathbf{v}'_i \mathbf{v}'_i^T$$

where  $\mathbf{v}'_i = \mathbf{v}_i - \mathbf{c}$ , and the eigenvectors  $\hat{\mathbf{d}}_1, \hat{\mathbf{d}}_2, \hat{\mathbf{d}}_3$  of  $C$  form the rotation matrix  $R = [\hat{\mathbf{d}}_1 \ \hat{\mathbf{d}}_2 \ \hat{\mathbf{d}}_3]$

Then, we convert the rotation matrix  $R$  into Euler angles  $(\phi, \theta, \psi)$ , which represent rotations around the x-, y-, and z-axes, respectively.

**Scaling.** The scaling factors  $l_1, l_2, l_3$  are the extents of the bounding box along the principal axes (given by the eigenvectors). These represent the lengths along each principal axis.

$$l_1 = \text{extent along } \hat{\mathbf{d}}_1, l_2 = \text{extent along } \hat{\mathbf{d}}_2, l_3 = \text{extent along } \hat{\mathbf{d}}_3$$

## Node Definitions

Following (Raistrick et al. 2023), we identified and translated 79 unique nodes from Blender’s geometry nodes into intuitive text representations that are both human-readable and machine-interpretable. Some key node types include:

- **Input:** Defines input parameters for PCG. These parameters are semantically defined by the variables corresponding to the specific parts they modify.
- **Mesh Primitives:** Basic geometric shapes that serve as building blocks for models.
  - *cube*: Creates a unit cube centered at the origin, with default sides of length 1 along each axis.
  - *cylinder*: Generates a cylinder aligned along the z-axis with specified radius and depth
  - *sphere*: Produces a sphere centered at the origin with a default radius value of 1
- **Transform:** Operations to manipulate geometry.
  - $T(x, y, z)$ : Moves geometry by the specified vector  $\mathbf{t} = (x, y, z)$ .
  - $R(rx, ry, rz)$ : Rotates geometry using Euler angles around the x-, y-, and z-axes by angles  $r_x, r_y$ , and  $r_z$ , respectively.
  - $S(s_x, s_y, s_z)$ : Scales geometry along the specified axes.

- **Geometry Operations:** Combine or modify meshes based on spatial relationships.
  - *join*: Combines the output of two or more geometry nodes into a single unified structure, represented as the union  $\mathcal{M} = \mathcal{M}_1 \cup \mathcal{M}_2 \cup \dots$
  - *switch*: Allows conditional selection between different geometries or operations based on a boolean input. This enables toggling parts of the model on or off.
  - *combine*: Merges separate scalar values into a vector. For instance, combining individual  $x$ ,  $y$ , and  $z$  components into a single position vector.
  - *extrude*: Extends geometry along its normals by a specified distance.
- **Math Operations:** Perform arithmetic operations on numerical inputs or attributes, often used for parametric controls.
  - *add*: Computes the sum of two inputs, such as adding two scalar values, vectors, or attributes.
  - *subtract*: Subtracts one input from another, typically used for adjusting positions, sizes, or other attributes.
  - *multiply*: Multiplies two inputs, often used for scaling or other proportional adjustments.
  - *divide*: Divides one input by another, useful for normalizing values or adjusting parameters.
- **Output:** Defines the output of the procedural graph.

## Experiments

**3D Generation.** We show qualitative comparison with 3DPremise (Yuan et al. 2024), an LLM-driven 3D generation method in Figure 10, and PerSel for 3D editing in Figure 11. Our method demonstrate improvements both in the quality of the generated 3D models and the time required to edit them. Proc3D enables the effectiveness in producing more detailed and realistic 3D models while enabling faster and more intuitive editing workflows compared to existing methods.

We further show several examples of the 3D models generated by Proc3D in Figure 12, and Figure 13

**3D Editing.** Figures 14, 15, and 16 demonstrate the process of editing the generated 3D models, showing how different modifications can be applied to refine the 3D structure, adjust components, and enhance their overall design. These figures highlight the effectiveness of our approach in enabling intuitive and precise 3D editing.

**Ablation Studies.** We further ablate LLaMA-3 70B and GPT-4o to assess the effect of ICL example count on PCG quality. Due to its 8K token limit, LLaMA-3 was constrained to 20 ICL examples from chair and table categories (avg. 302 tokens each), while GPT-4o’s 128K context allowed up to 300. Results in Figure 9 show rapid performance gains up to 20 examples, after which improvements plateau, suggesting an effective ICL threshold. These findings reinforce that the PCG representation allows strong compositional reasoning from limited demonstrations.

## Conclusion

We presented Proc3D, a method for generation and real-time editing of 3D models. Our approach advances generation of 3D models from LLMs by generating higher-quality models and enabling faster, more intuitive editing workflows. Despite limitations due to dataset constraints and the use of a single cube primitive, Proc3D represents a step toward more efficient and user-friendly 3D modeling. Future work will aim to address these challenges to enhance the system’s robustness and applicability.

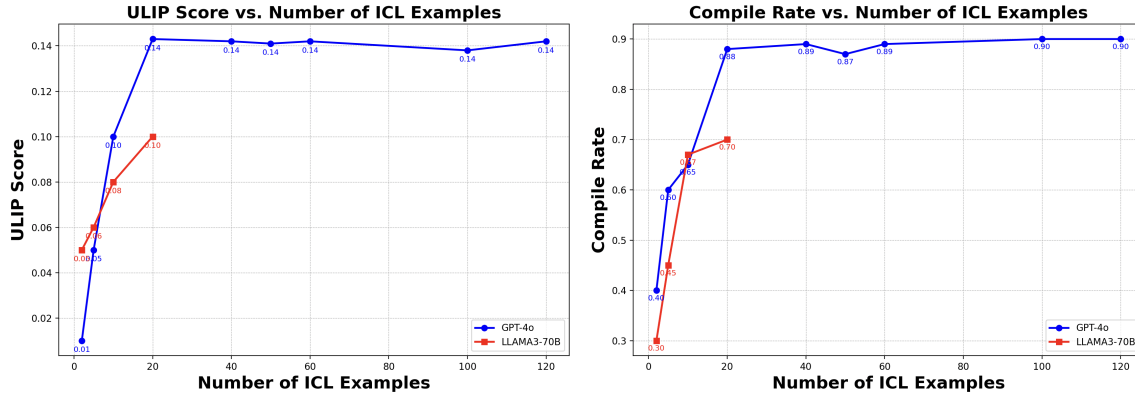


Figure 9: **Ablation Study on ICL Examples for 3D Model Generation.** Results show performance improvements up to 20 examples, with no major improvement thereafter, indicating an optimal threshold for model performance in PCG generation.

Table 4: **Compilation Efficiency Comparison Across Reasoning Models.** We compare different procedural representations evaluated using reasoning-oriented LLMs (o3, and DeepSeek-V3). Our PCG representation achieves the highest compile rate (CR) while substantially reducing token count and generation time on both o3 and DeepSeek-V3 reasoning models.

Representation	o3 (Reasoning Model)			DeepSeek-V3 (Reasoning Model)		
	CR (%)	Tokens	Time (s)	CR (%)	Tokens	Time (s)
Blender Geometry Nodes	0	6035	420	0	6027	279
Infinigen DSL	15	3270	238	9	3190	225
Blender Python	65	2660	151	63	2585	194
<b>PCG (Ours)</b>	<b>94</b>	<b>655</b>	<b>73</b>	<b>92</b>	<b>689</b>	<b>61</b>

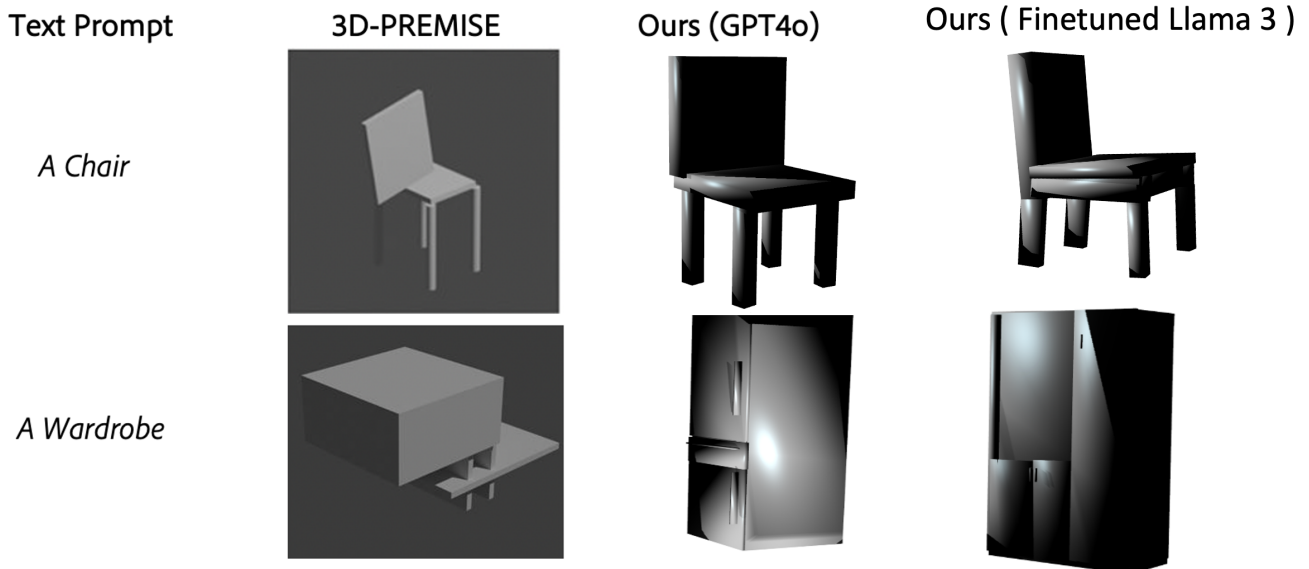


Figure 10: **Qualitative Comparison with LLM-Driven 3D method.** Our method shows improvement over 3DPremise (Yuan et al. 2024), which uses native blender’s code for 3D object generation.

Method	Edit Instruction	Input shape	Output shape	Inference Latency
ParSEL	<i>Shorten the Legs</i>			30 – 500 seconds
Ours (GPT4o)	<i>Shorten the Legs</i>			< 10ms

Figure 11: **Quatitative Comparison with LLM-Driven 3D Editing method.** Our method shows improvement over ParSEL (Ganeshan et al. 2024) which directly edits 3D mesh representation.

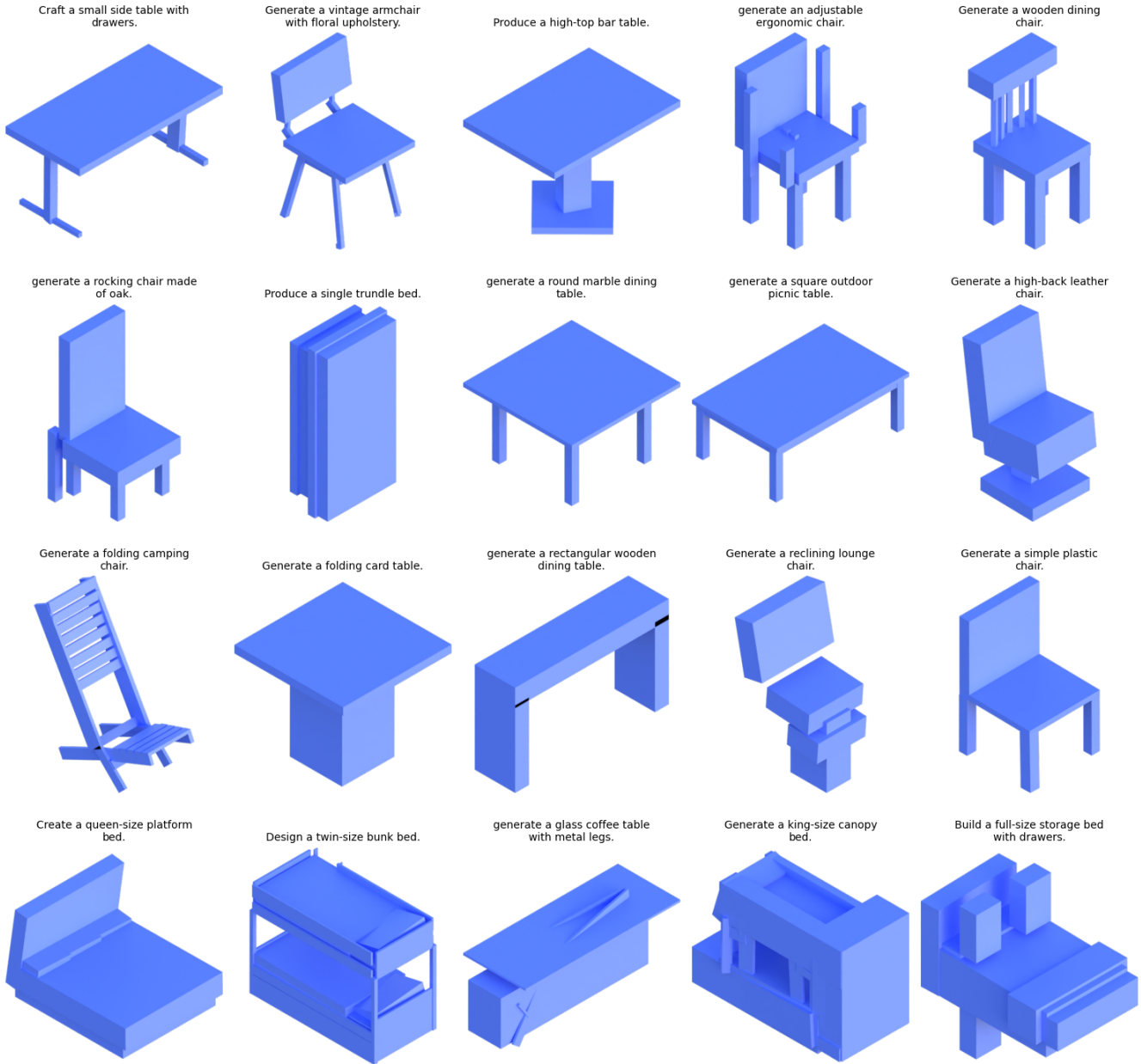


Figure 12: **Qualitative Examples of the Proc3D system from uniquely generated text prompts.** These are examples of the randomly sampled prompts used for all quantitative experiments in the main paper.

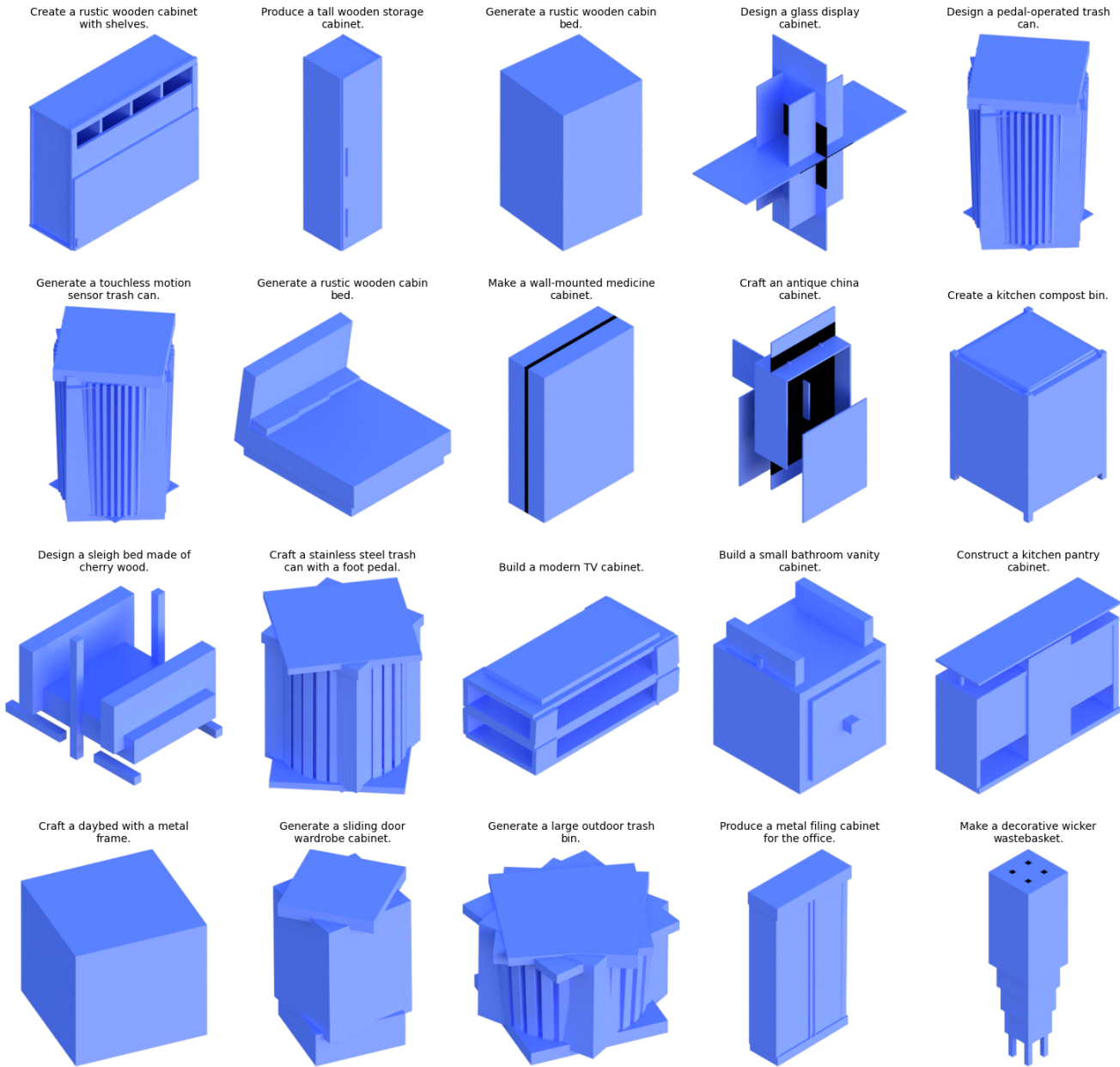
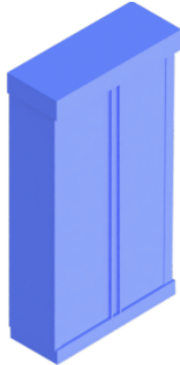
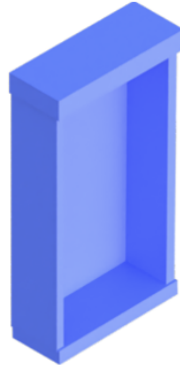


Figure 13: **Qualitative Examples of the Proc3D system from uniquely generated text prompts.** These are examples of the randomly sampled prompts used for all quantitative experiments in the main paper.

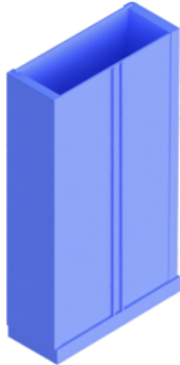
Produce a metal filing cabinet for the office.



Open the door



Close the door and remove the top panel



Design a pedal-operated trash can.



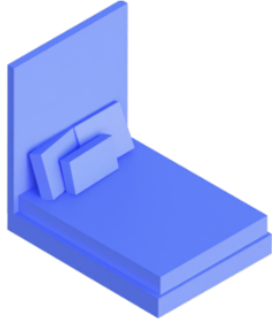
I can see a box inside, remove it



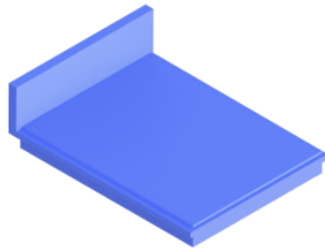
Now remove the cover



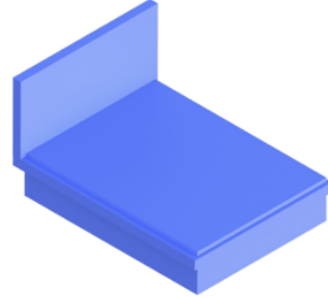
Create a modern upholstered bed with a tall headboard.



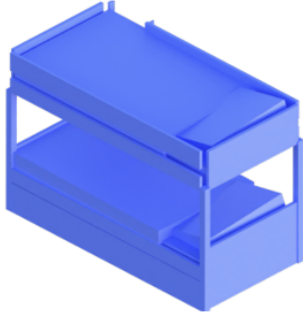
I like this bed, but i dont like the pillows, i also want to reduce the height of the back



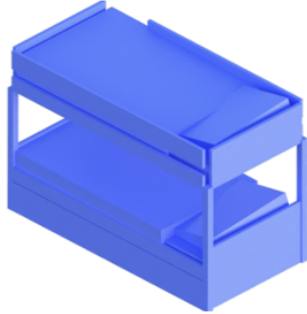
Now increase thisickness of the bed frame



Design a twin-size bunk bed.



Remove the ladder



Remove all blankets



Figure 14: **Qualitative Editing Results of Proc3D.** Proc3D can precisely edit the generated 3D models

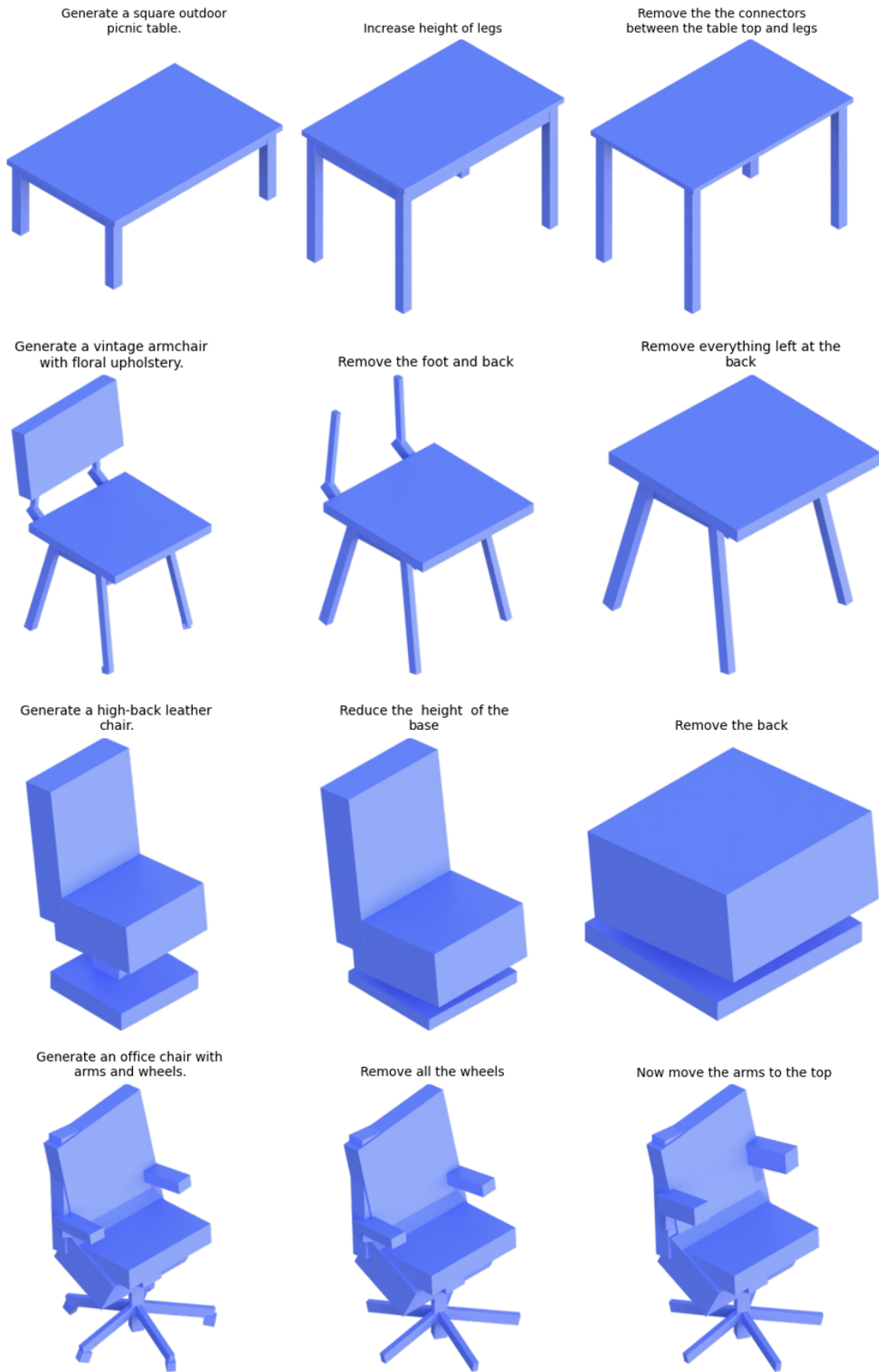


Figure 15: **Qualitative Editing Results of Proc3D.** Proc3D can precisely edit the generated 3D models

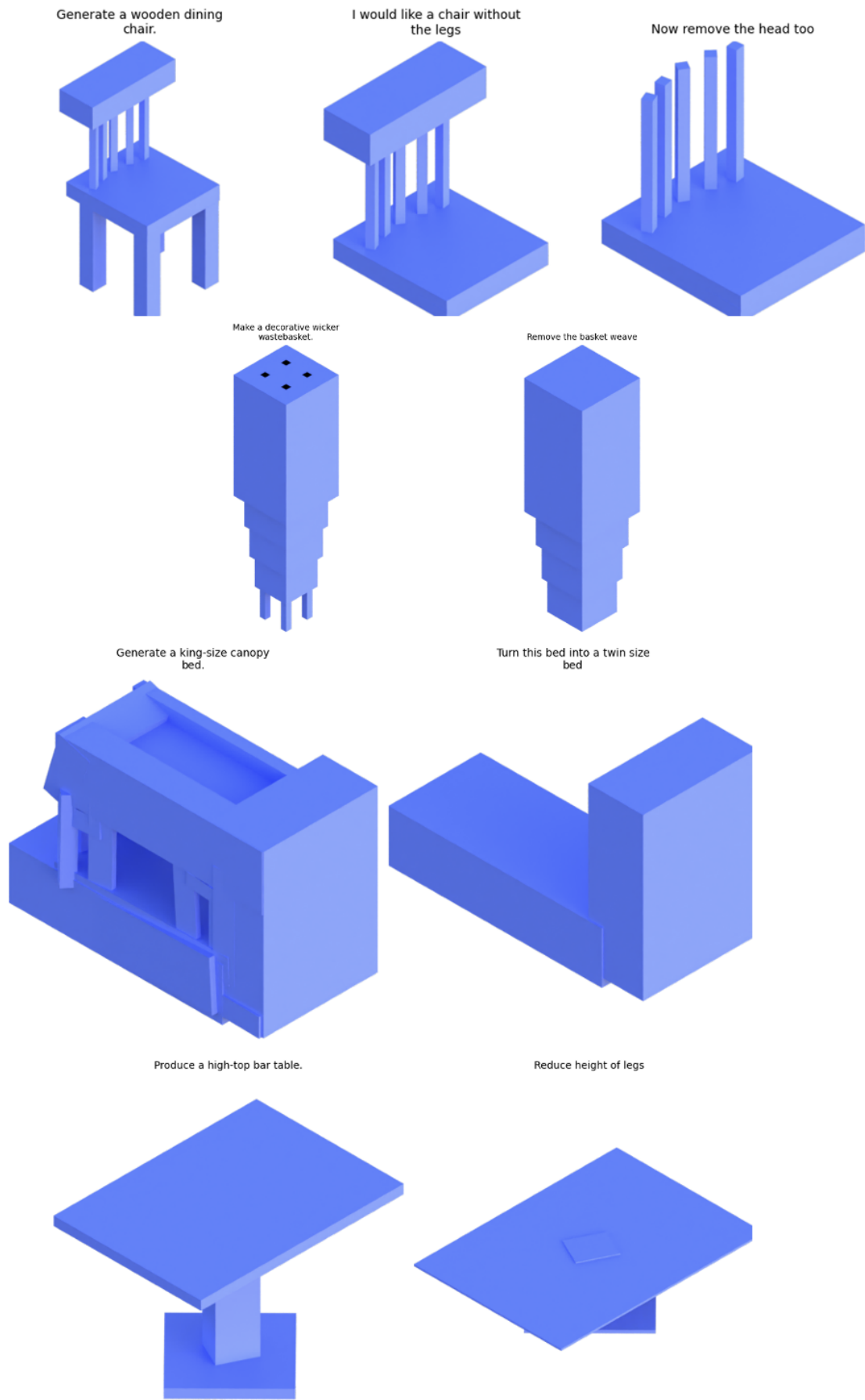


Figure 16: **Qualitative Editing Results of Proc3D.** Proc3D can precisely edit the generated 3D models

```

1 def extract(obj_filename):
2     obj = load_object(obj_filename)
3     boxes = obj.boxes(leafs_only=True)
4
5     current_tokens = {"inputs": {"Geometry": "cube"}}
6     created_vectors = {"vector_counts": {}}
7     done = {}
8     switches = {}
9
10    for node in obj.depth_first_traversal():
11        if node.is_leaf:
12            box = node.box
13            box[:3] = coord_rot @ box[:3]
14            box[6:9] = coord_rot @ box[6:9]
15            box[9:] = coord_rot @ box[9:]
16
17            T, R, S = extract_transformations(box)
18            names = clean_path(node.full_label)
19
20            # Traverse and build hierarchy graph
21            current = done
22            for i, name in enumerate(names):
23                if name not in current:
24                    current[name] = [] if i == len(names)-2 else {}
25                    current = current[name]
26
27            token, graph_str = attach_part(name, (T, R, S), current_tokens,
28                                            created_vectors, switches)
29            current.append(token)
30
31            switch_str, changed_tokens = join_all_switches(switches, current_tokens)
32            token, graph_str2 = recursively_join(done, changed_tokens, current_tokens)
33
34            token, graph_str3 = expose_rotation(global_name, token, current_tokens)
35
36            output = format_output(token, switch_str + graph_str2, current_tokens, created_vectors)
37            save_graph(output, obj_filename)

```

Figure 17: Extracting Transformation and Composing Graph from PartNet Dataset

```

1 # Example Python code
2 import bpy
3 import mathutils
4 from numpy.random import uniform, normal, randint
5 from infinigen.core.nodes.node_wrangler import Nodes, NodeWrangler
6 from infinigen.core.nodes import node_utils
7 from infinigen.core.util.color import color_category
8 from infinigen.core import surface
9
10 def geometry_nodes(nw: NodeWrangler):
11     # Code generated using version 2.6.5 of the node_transpiler
12
13     group_input = nw.new_node(Nodes.GroupInput,
14         expose_input=[('NodeSocketGeometry', 'Geometry', None),
15             ('NodeSocketFloatDistance', 'TableWidth', 2.0000),
16             ('NodeSocketFloatDistance', 'TableHeight', 2.0000),
17             ('NodeSocketFloatDistance', 'TopCurve', 0.2500),
18             ('NodeSocketFloat', 'TopThickness', 1.0000),
19             ('NodeSocketFloatDistance', 'LegRadius', 1.0000),
20             ('NodeSocketFloatDistance', 'LegHeight', 2.0000)])
21
22     subtract = nw.new_node(Nodes.Math, input_kwargs={0: group_input.outputs["TableWidth"]}, attrs={'operation': 'SUBTRACT'})
23
24     subtract_1 = nw.new_node(Nodes.Math, input_kwargs={0: group_input.outputs["TableHeight"]}, attrs={'operation': 'SUBTRACT'})
25
26     quadrilateral_1 = nw.new_node(Nodes.Quadrilateral, input_kwargs={'Width': subtract, 'Height': subtract_1})
27
28     cylinder = nw.new_node(Nodes.Cylinder,
29         input_kwargs={'Radius': group_input.outputs["LegRadius"], 'Depth': group_input.outputs["LegHeight"]})
30
31     instance_on_points = nw.new_node(Nodes.InstanceOnPoints, input_kwargs={'Points': quadrilateral_1, 'Instance': cylinder.outputs["Mesh"]})
32
33     divide = nw.new_node(Nodes.Math,
34         input_kwargs={0: group_input.outputs["LegHeight"], 1: -2.0000}, attrs={'operation': 'DIVIDE'})
35
36     combine_xyz = nw.new_node(Nodes.CombineXYZ, input_kwargs={'Z': divide})
37
38     transform_geometry = nw.new_node(Nodes.Transform, input_kwargs={'Geometry': instance_on_points, 'Translation': combine_xyz})
39
40     quadrilateral = nw.new_node(Nodes.Quadrilateral,
41         input_kwargs={'Width': group_input.outputs["TableWidth"], 'Height': group_input.outputs["TableHeight"]})
42
43     fillet_curve = nw.new_node(Nodes.FilletCurve,
44         input_kwargs={'Curve': quadrilateral, 'Count': 20, 'Radius': group_input.outputs["TopCurve"]})
45
46     fill_curve = nw.new_node(Nodes.FillCurve, input_kwargs={'Curve': fillet_curve}, attrs={'mode': 'NGONS'})
47
48     extrude_mesh = nw.new_node(Nodes.ExtrudeMesh,
49         input_kwargs={'Mesh': fill_curve, 'Offset Scale': group_input.outputs["TopThickness"]})
50
51     join_geometry = nw.new_node(Nodes.JoinGeometry,
52         input_kwargs={'Geometry': [transform_geometry, fillet_curve, extrude_mesh.outputs["Mesh"]]}))
53
54     group_output = nw.new_node(Nodes.GroupOutput, input_kwargs={'Geometry': join_geometry}, attrs={'is_active_output': True})
55
56     def apply(obj, selection=None, **kwargs):
57         surface.add_geomod(obj, geometry_nodes, selection=selection, attributes[])

```

Figure 18: Infinigen Blender Python Code for Creating a Table Model